PERGAMON

International Journal of Solids and Structures 38 (2001) 2305–2321

INTERNATIONAL JOURNAL OF SOLIDS and STRUCTURES

www.elsevier.com/locate/ijsolstr

Differential quadrature element method for buckling analysis of rectangular Mindlin plates having discontinuities

F.-L. Liu *

CAD/CAM Laboratory, School of Mechanical and Production Engineering, Nanyang Technological University, North Spine (N3) Level 2, Nanyang Avenue, 639798 Singapore, Singapore

Received 19 February 1999; in revised form 20 March 2000

Abstract

In this paper, a new solution approach, the differential quadrature element method is applied to the buckling analysis of discontinuous rectangular plates based on the Mindlin plate theory. The domain decomposition method is used to divide the solution domain into smaller elements according to the discontinuities contained in the plate. Then, differential quadrature procedures are applied to each element to formulate the discretized element governing equations. These discrete equations are then assembled into an overall equation system, using the compatibility conditions, and solved by a standard eigensolver. Detailed formulations for modeling of the plate and the compatibility conditions are derived. Convergence and comparison studies are carried out to examine the reliability and accuracy of the numerical solutions. Four rectangular Mindlin plates with different discontinuities (mixed boundary conditions and cracks) are analyzed to show the applicability and flexibility of the present methodology for solving a class of buckling problems. Due to the lack of published solutions for buckling of thick discontinuous plates and the high accuracy of the present approach, the solutions obtained may serve as benchmark values for further studies. © 2001 Published by Elsevier Science Ltd.

Keywords: Differential quadrature element method; Mindlin plate; Buckling analysis; Plates with discontinuities; Numerical method

1. Introduction

Elastic buckling problems of moderately thick rectangular plates have been studied by many researchers. Srinivas and Rao (1969) presented an exact three-dimensional analysis for the buckling of simply supported thick rectangular plates. Brunelle (1971) treated the elastic stability of transversely isotropic Mindlin plates with two parallel sides simply supported and the other sides arbitrarily constrained. Brunelle and Robertson (1974) derived the governing equations of a transversely isotropic, initially stressed Mindlin plate, and solved the thick plate equations for a simply supported rectangular plate under the combination action of a uniform compressive stress and a uniform bending stress acting in the same direction. Rao et al. (1975) analyzed the stability of moderately thick rectangular plates by using a high precision triangular finite

* Tel.: +65-799-5557/6906; fax: +65-791-1859.
E-mail address: mfllliu@ntu.edu.sg (F.-L. Liu).

0020-7683/01/$ - see front matter © 2001 Published by Elsevier Science Ltd.
PII: S0020-7683(00)00120-7

element. Hinton (1978) studied the buckling of initially stressed Mindlin plates by the finite strip method, and obtained some results for plates with two opposite sides simply supported and various support conditions on the other sides. Luo (1982) performed the finite element analysis for the buckling of thin and moderately thick plates using a hybrid/mixed finite element. Dawe and Roufaeil (1982) solved the elastic buckling problem of rectangular Mindlin plates using both the finite strip method and the Rayleigh–Ritz method. In the above studies, only the elastic buckling of continuous Mindlin plates with uniform boundaries has been considered.

Regarding the buckling of rectangular plates with discontinuities, Hamada et al. (1967) analyzed thin rectangular plates with simply supported but partially clamped edges. Keer and Stahl studied simply supported rectangular thin plates having mixed boundary conditions (Keer and Stahl, 1972) and cracks (Stahl and Keer, 1972) using an analytical approach. Sakiyama and Matsuda (1987) analyzed the buckling of rectangular Mindlin plates with mixed boundary conditions using an approximate method. However, only the solutions for thin plates ($h/a = 0.01$) with mixed boundary conditions were presented. In the open literature, solutions to the buckling of discontinuous thick plates are scarce. The objective of the present paper is to apply and demonstrate a new numerical solution approach, the differential quadrature element method, to determine the buckling loads of thick rectangular plates having various discontinuities.

The differential quadrature method was originated by Bellman and his associates (Bellman and Casti, 1971; Bellman et al., 1972) for solving linear and nonlinear differential equations. It was first introduced to the structural analysis field by Bert and his associates (Bert et al., 1988, 1989; Striz et al., 1988). Since then, there have been numerous developments and applications of the method in solid and structural mechanics. An excellent review paper by Bert and Malik (1996) presented a detailed literature list on both the numerical development and the engineering application aspects of this method. All of the analyzes yielded good to excellent solutions. However, further application of the method has been greatly restricted by the disadvantage that it cannot be directly employed to solve problems with discontinuities. To overcome this drawback, Striz et al. developed the quadrature element method (QEM) to perform static and vibration analyzes of trusses, beams, and thin plates by combining a domain decomposition method with the differential quadrature method (Striz et al., 1994, 1997; Chen et al., 1997). Wang and Gu (1997) developed a one-dimensional differential quadrature element method for beam, column, and frame structure analysis. Han and Liew (1996) also developed a one-dimensional differential quadrature element method for bending analysis of axisymmetric circular Mindlin plates. The present author developed the two-dimensional differential quadrature element method for static and vibration analyzes of discontinuous thick plate problems (Liu and Liew, 1998, 1999a,b,c; Liu, 2000). The differences between the quadrature element method and the differential quadrature element method have been elaborated in previous publications by Wang and Gu (1997) and Liu (2000). In this paper, the two-dimensional differential quadrature element method is further extended to the buckling analysis of rectangular Mindlin plates. The plates considered here are described by the first-order shear deformation theory (Mindlin plate theory) and composed of isotropic material.

2. Mathematical formulations

2.1. Governing differential equations

Consider a rectangular Mindlin plate with dimensions $a \times b$ and subjected to uniform in-plane loads P_x and P_y. This plate is divided into N_E elements based on the discontinuities in the geometry, boundary constraints, and materials used. Each element consists of an isotropic material and has uniform thickness and continuous boundary constrains on each edge. For a given element l, the governing differential equations for buckling of the isotropic shear deformable plate are given according to Leissa (1995) and Whitney (1987) as follows:

$$\frac{\partial^2\psi_x}{\partial x^2}+\frac{(1-v_l)}{2}\frac{\partial^2\psi_x}{\partial y^2}+\frac{(1+v_l)}{2}\frac{\partial^2\psi_y}{\partial x\partial y}-\frac{\kappa G_l h_l}{D_l}\left(\frac{\partial w}{\partial x}+\psi_x\right)=0, \tag{1a}$$

$$\frac{(1+v_l)}{2}\frac{\partial^2\psi_x}{\partial x\partial y}+\frac{\partial^2\psi_y}{\partial y^2}+\frac{(1-v_l)}{2}\frac{\partial^2\psi_y}{\partial x^2}-\frac{\kappa G_l h_l}{D_l}\left(\frac{\partial w}{\partial y}+\psi_y\right)=0, \tag{1b}$$

$$\left(\frac{\partial^2 w}{\partial x^2}+\frac{\partial^2 w}{\partial y^2}\right)+\left(\frac{\partial\psi_x}{\partial x}+\frac{\partial\psi_y}{\partial y}\right)=\frac{1}{\kappa G_l h_l}\left[P_x\frac{\partial^2 w}{\partial x^2}+P_y\frac{\partial^2 w}{\partial y^2}\right], \tag{1c}$$

where w, ψ_x, and ψ_y are the transverse deflection, the rotation of the normal about the y-axis and the rotation of the normal about the x-axis, respectively; h_l, E_l, G_l, and v_l are the thickness of the plate, Young's modulus, shear modulus, and Poisson's ratio, respectively; D_l is the plate flexural rigidity; and κ is the shear correction factor. Reissner (1945) used $5/6$ as the value of κ, whereas Mindlin (1951) employed $\pi^2/12$ as the shear correction factor. Wittrick (1987) found that the value of κ should be $5/(6-v)$ through some very detailed analytical investigations on the exact solutions of the elasticity equations and the Mindlin theory for simply supported plates. Malik and Bert (1998) made a comprehensive compartive study for the effects of the κ value on the numerical results of free vibration problems for thick rectangular plates and showed that Wittrick's correction factor leads to more accurate results for thick plates than Reissner's correction factor and Mindlin's factor. Therefore, in the present study, the value of κ, unless specified, is taken to be $\kappa=5/(6-v)$.

The moments and shear forces are expressed as

$$M_x=D_l\left(\frac{\partial\psi_x}{\partial x}+v_l\frac{\partial\psi_y}{\partial y}\right), \tag{2a}$$

$$M_y=D_l\left(v_l\frac{\partial\psi_x}{\partial x}+\frac{\partial\psi_y}{\partial y}\right), \tag{2b}$$

$$M_{xy}=\frac{1-v_l}{2}D_l\left(\frac{\partial\psi_x}{\partial y}+\frac{\partial\psi_y}{\partial x}\right), \tag{2c}$$

$$Q_x=\kappa G_l h_l\left(\frac{\partial w}{\partial x}+\psi_x\right), \tag{2d}$$

$$Q_y=\kappa G_l h_l\left(\frac{\partial w}{\partial y}+\psi_y\right). \tag{2e}$$

The boundary conditions considered herein are divided into three kinds. For example, for an edge with $x=$ constant, they are

(a) *Clamped edge (C)*

$$w=0,\quad \psi_x=0,\quad \psi_y=0. \tag{3a–c}$$

(b) *Simply supported edge (S)*

$$w=0,\quad \psi_y=0,\quad M_x=0. \tag{4a–c}$$

(c) *Free edge (F)*

$$Q_x-P_x\frac{\partial w}{\partial x}=0,\quad M_x=0,\quad M_{xy}=0. \tag{5a–c}$$

2.2. Discretization of governing equations for rectangular Mindlin differential quadrature plate buckling element

The lth element is further divided into $N_x \times N_y$ grid points in the x- and y-directions, respectively (Liu and Liew, 1998, 1999b). Using differential quadrature method procedures (Liew et al., 1996; Bert and Malik, 1996), the discrete governing equations for elastic buckling of the lth plate element can be discretized at each discrete point of the inner mesh into

$$\sum_{k=1}^{N_{lx}} C_{ik}^{(2)}(\psi_x)_{kj} + \frac{(1-\nu_l)}{2}\sum_{m=1}^{N_{ly}} \bar{C}_{jm}^{(2)}(\psi_x)_{im} - \frac{\kappa G_l h_l}{D_l}(\psi_x)_{ij} + \frac{(1+\nu_l)}{2}\left[\sum_{k=1}^{N_{lx}} C_{ik}^{(1)}\sum_{m=1}^{N_{ly}} \bar{C}_{jm}^{(1)}(\psi_y)_{km}\right] - \frac{\kappa G_l h_l}{D_l}\sum_{k=1}^{N_{lx}} C_{ik}^{(1)}(w)_{kj} = 0, \tag{6a}$$

$$\frac{(1+\nu_l)}{2}\left[\sum_{k=1}^{N_{lx}} C_{ik}^{(1)}\sum_{m=1}^{N_{ly}} \bar{C}_{jm}^{(1)}(\psi_x)_{km}\right] + \sum_{m=1}^{N_{ly}} \bar{C}_{jm}^{(2)}(\psi_y)_{im} + \frac{(1-\nu_l)}{2}\sum_{k=1}^{N_{lx}} C_{ik}^{(2)}(\psi_y)_{kj} - \frac{\kappa G_l h_l}{D_l}(\psi_y)_{ij} - \frac{\kappa G_l h_l}{D_l}\sum_{m=1}^{N_{ly}} \bar{C}_{jm}^{(1)}(w)_{im} = 0, \tag{6b}$$

$$\sum_{k=1}^{N_{lx}} C_{ik}^{(2)}(w)_{kj} + \sum_{m=1}^{N_{ly}} \bar{C}_{jm}^{(2)}(w)_{im} + \sum_{k=1}^{N_{lx}} C_{ik}^{(1)}(\psi_x)_{kj} + \sum_{m=1}^{N_{ly}} \bar{C}_{jm}^{(1)}(\psi_y)_{im} = \frac{1}{\kappa G_l h_l}\left[P_x\sum_{k=1}^{N_{lx}} C_{ik}^{(2)}(w)_{kj} + P_y\sum_{m=1}^{N_{ly}} \bar{C}_{jm}^{(2)}(w)_{im}\right], \quad i = 1,2,3,\ldots,N_x,\ \ j = 1,2,3,\ldots,N_y, \quad l = 1,2,3,\ldots,N_E, \tag{6c}$$

where $C_{rs}^{(n)}$ and $\bar{C}_{rs}^{(n)}$ $(r = 1,2,3,\ldots,N_x; s = 1,2,3,\ldots,N_y)$ are the weighting coefficients for the nth-order partial derivatives of w, ψ_x, and ψ_y with respect to the global co-ordinates x and y.

Similarly, the moments and shear forces can be discretized as

$$(M_x)_{ij} = D_l\left[\sum_{k=1}^{N_x} C_{ik}^{(1)}(\psi_x)_{kj} + \nu_l\sum_{m=1}^{N_y} \bar{C}_{jm}^{(1)}(\psi_y)_{im}\right], \tag{7a}$$

$$(M_y)_{ij} = D_l\left[\sum_{m=1}^{N_y} \bar{C}_{jm}^{(1)}(\psi_y)_{im} + \nu_l\sum_{k=1}^{N_x} C_{ik}^{(1)}(\psi_x)_{kj}\right], \tag{7b}$$

$$(M_{xy})_{ij} = \frac{(1-\nu_l)}{2}D_l\left[\sum_{m=1}^{N_y} \bar{C}_{jm}^{(1)}(\psi_x)_{im} + \sum_{k=1}^{N_x} C_{ik}^{(1)}(\psi_y)_{kj}\right], \tag{7c}$$

$$(Q_x)_{ij} = \kappa G_l h_l\left[(\psi_x)_{ij} + \sum_{k=1}^{N_x} C_{ik}^{(1)} w_{kj}\right], \tag{7d}$$

$$(Q_y)_{ij} = \kappa G_l h_l\left[(\psi_y)_{ij} + \sum_{m=1}^{N_y} \bar{C}_{jm}^{(1)} w_{im}\right]. \tag{7e}$$

At the four edges of element l, the corresponding boundary conditions or compatibility conditions should be used. If the edge is located at a side of the plate, the boundary conditions (3)–(5) are used, otherwise, the compatibility conditions should be employed. Taking the edge $x = 0$ of the element l for example, the boundary conditions can be discretized into the following forms:

$$\text{(S)} \quad w_{1j} = 0, \quad j = 1, 2, \ldots, N_y, \tag{8a}$$

$$\sum_{k=1}^{N_x} C_{1k}^{(1)} (\psi_x)_{kj} + v_l \sum_{m=1}^{N_y} \bar{C}_{jm}^{(1)} (\psi_y)_{1m} = 0, \quad j = 1, 2, \ldots, N_y, \tag{8b}$$

$$(\psi_y)_{1j} = 0, \quad j = 1, 2, \ldots, N_y, \tag{8c}$$

$$\text{(C)} \quad w_{1j} = 0, \quad j = 1, 2, \ldots, N_y, \tag{9a}$$

$$(\psi_x)_{1j} = 0, \quad j = 1, 2, \ldots, N_y, \tag{9b}$$

$$(\psi_y)_{1j} = 0, \quad j = 1, 2, \ldots, N_y, \tag{9c}$$

$$\text{(F)} \quad \kappa G_l h_l \left[\sum_{k=1}^{N_x} C_{1k}^{(1)} w_{kj} + (\psi_x)_{1j} \right] - P_x \sum_{k=1}^{N_x} C_{1k}^{(1)} w_{kj} = 0, \quad j = 1, 2, \ldots, N_y, \tag{10a}$$

$$\sum_{k=1}^{N_x} C_{1k}^{(1)} (\psi_x)_{kj} + v_l \sum_{m=1}^{N_y} \bar{C}_{jm}^{(1)} (\psi_y)_{1m} = 0, \quad j = 1, 2, \ldots, N_y, \tag{10b}$$

$$\sum_{m=1}^{N_y} \bar{C}_{jm}^{(1)} (\psi_x)_{1m} + \sum_{k=1}^{N_x} C_{1k}^{(1)} (\psi_y)_{kj} = 0, \quad j = 1, 2, \ldots, N_y. \tag{10c}$$

Eqs. (6a)–(6c) can be expressed in matrix form as

$$\mathbf{K}^{\mathrm{e}} \mathbf{d}^{\mathrm{e}} = p^2 \mathbf{B}^{\mathrm{e}} \mathbf{d}^{\mathrm{e}}, \tag{11}$$

where $p^2 = P_x b^2/(\pi^2 D)$ is defined as the buckling factor; $\mathbf{K}^{\mathrm{e}}$, $\mathbf{d}^{\mathrm{e}}$, and $\mathbf{B}^{\mathrm{e}}$ are the element weighting coefficient matrix, element displacement vector, and element force matrix, respectively. And

$$\mathbf{d}^{\mathrm{e}} = [w_{1,1}, \psi_{x1,1}, \psi_{y1,1}, w_{1,2}, \psi_{x1,2}, \psi_{y1,2}, \ldots, w_{N_x,N_y}, \psi_{xN_x,N_y}, \psi_{yN_x,N_y}]^{\mathrm{T}}, \tag{12}$$

$$\mathbf{B}^{\mathrm{e}} = [\mathbf{b}_{1,1}^{\mathrm{e}}, \mathbf{b}_{1,2}^{\mathrm{e}}, \ldots, \mathbf{b}_{1,N_y}^{\mathrm{e}}, \mathbf{b}_{2,1}^{\mathrm{e}}, \mathbf{b}_{2,2}^{\mathrm{e}}, \ldots, \mathbf{b}_{2,N_y}^{\mathrm{e}}, \ldots, \mathbf{b}_{N_x,1}^{\mathrm{e}}, \ldots, \mathbf{b}_{N_x,N_y}^{\mathrm{e}}]^{\mathrm{T}}, \tag{13}$$

where $\mathbf{b}_{1,1}^{\mathrm{e}}, \mathbf{b}_{1,2}^{\mathrm{e}}, \ldots, \mathbf{b}_{1,N_y}^{\mathrm{e}}, \mathbf{b}_{2,1}^{\mathrm{e}}, \mathbf{b}_{2,2}^{\mathrm{e}}, \ldots, \mathbf{b}_{2,N_y}^{\mathrm{e}}, \ldots, \mathbf{b}_{N_x,1}^{\mathrm{e}}, \mathbf{b}_{N_x,2}^{\mathrm{e}}, \ldots, \mathbf{b}_{N_x,N_y}^{\mathrm{e}}$ are null matrices with $3N \times 3$ elements, and $\mathbf{b}_{2,2}^{\mathrm{e}}, \ldots, \mathbf{b}_{2,N_y-1}^{\mathrm{e}}, \ldots, \mathbf{b}_{N_x-1,2}^{\mathrm{e}}, \ldots,$ and $\mathbf{b}_{N_x-1,N_y-1}^{\mathrm{e}}$ are matrices with $3N \times 3$ elements, in which only one element at the corresponding point in each matrix is not equal to zero, the other elements are all zeros. Taking matrix $\mathbf{b}_{2,2}^{\mathrm{e}}$, for instance, it can be expressed as

$$\mathbf{b}^{e}_{2,2} = \begin{bmatrix} \overbrace{0,0,0,\ldots,0,0,0,}^{j=1,2,3,\ldots,3N_y} & \overbrace{0,0,0,0,0,0,\ldots,0,0,0,}^{j=3N_y+1,3N_y+2,3N_y+3,\ldots,6N_y} & \overbrace{0,0,0,\ldots,0,0,0}^{j=6N_y+1,6N_y+2,\ldots,3N} \\ 0,0,0,\ldots,0,0,0, & 0,0,0,0,0,0,\ldots,0,0,0, & 0,0,0,\ldots,0,0,0 \\ 0,0,0,\ldots,0,0,0, & 0,0,0,\frac{P_x\left(C^{(2)}_{22}+\beta\bar{C}^{(2)}_{22}\right)}{\kappa G_l h_l},0,0,\ldots,0,0,0, & 0,0,0,\ldots,0,0,0 \end{bmatrix}. \tag{14}$$

The coefficients in $\mathbf{K}^e$ are determined by Eqs. (6a)–(6c).

2.3. Compatibility conditions for connection of plate elements

To obtain solutions, the discrete element weighting coefficient matrices, element displacement vectors, and element force matrices should be assembled together. Therefore, compatibility conditions for the connection of plate elements need to be established. Since the same global nodal number is used for each conjunction node at the interface boundaries of elements, the displacement compatibility conditions are automatically satisfied at all the interface conjunction nodes. Only the equilibrium conditions are needed. Following the same procedures as in previous studies (Liu and Liew, 1998, 1999a,b), the compatibility conditions for buckling analysis can be derived. It is found that they are the same as those for the vibration analysis of Mindlin plates (Liu and Liew, 1999b). Hence, according to the locations of the conjunction nodes, the compatibility conditions for the buckling of Mindlin plates are given below.

- For conjunction nodes at which two elements meet. As shown in Fig. 1(a), the compatibility conditions for a conjunction node at which two elements l_1 and l_2 are connected in the x direction are

$$(Q_x^{l_1})_{N_x,j} - (Q_x^{l_2})_{1,j} = 0, \qquad (M_x^{l_1})_{N_x,j} - (M_x^{l_2})_{1,j} = 0, \qquad (M_{xy}^{l_1})_{N_x,j} - (M_{xy}^{l_2})_{1,j} = 0. \tag{15a–c}$$

  For a conjunction node at which two elements l_1 and l_2 are connected in the y-direction (Fig. 1(b)), the compatibility conditions become

$$(Q_y^{l_1})_{i,N_y} - (Q_y^{l_2})_{i,1} = 0, \qquad (M_y^{l_1})_{i,N_y} - (M_y^{l_2})_{i,1} = 0, \qquad (M_{xy}^{l_1})_{i,N_y} - (M_{xy}^{l_2})_{i,1} = 0. \tag{16a–c}$$

- For conjunction nodes at which four elements meet. If four adjacent elements l_1, l_2, l_3, and l_4 are connected at node m as shown in Fig. 1(c), we have the following compatibility conditions:

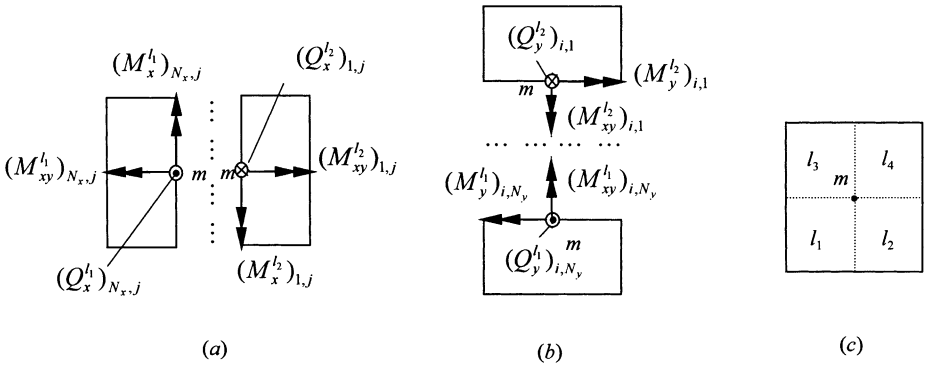

Fig. 1. Locations of conjunction nodes on the interface boundaries of adjacent elements: (a) two elements connected in x-direction, (b) two elements connected in y-direction, and (c) four elements connected.

$$(Q_x^{l_1})_{N_x,N_y} + (Q_x^{l_2})_{N_x,1} - (Q_x^{l_3})_{1,N_y} - (Q_x^{l_4})_{1,1} = 0, \tag{17a}$$

$$(M_x^{l_1})_{N_x,N_y} + (M_x^{l_2})_{N_x,1} - (M_x^{l_3})_{1,N_y} - (M_x^{l_4})_{1,1} = 0, \tag{17b}$$

$$(M_{xy}^{l_1})_{N_x,N_y} + (M_{xy}^{l_2})_{N_x,1} - (M_{xy}^{l_3})_{1,N_y} - (M_{xy}^{l_4})_{1,1} = 0 \tag{17c}$$

or

$$(Q_y^{l_1})_{N_x,N_y} - (Q_y^{l_2})_{N_x,1} + (Q_y^{l_3})_{1,N_y} - (Q_y^{l_4})_{1,1} = 0, \tag{18a}$$

$$(M_y^{l_1})_{N_x,N_y} - (M_y^{l_2})_{N_x,1} + (M_y^{l_3})_{1,N_y} - (M_y^{l_4})_{1,1} = 0, \tag{18b}$$

$$(M_{xy}^{l_1})_{N_x,N_y} - (M_{xy}^{l_2})_{N_x,1} + (M_{xy}^{l_3})_{1,N_y} - (M_{xy}^{l_4})_{1,1} = 0. \tag{18c}$$

The final global matrix form of the equation system for the entire plate becomes

$$\mathbf{Kd} = p^2\mathbf{Bd}, \tag{19}$$

where $\mathbf{K}$, $\mathbf{d}$, and $\mathbf{B}$ are the overall weighting coefficient matrix, global displacement vector, and overall force matrix of the plate.

3. Convergence and accuracy studies

The final equation matrix is a set of linear algebraic eigenvalue equations. Solving this equation system using an ordinary eigenvalue equation system solver, the solutions to the entire plate can be obtained. The grid points employed for the lth element in the computations are designated according to the Chebyshev grid spacing pattern as follows:

$$x_i = (x)_{i_e} + [(x)_{i_e+1} - (x)_{i_e}]\{1 - \cos[(i-1)\pi/(N_x-1)]\}/2, \quad i = 1,2,3,\ldots,N_x, \tag{20}$$

$$y_j = (y)_{j_e} + [(y)_{j_e+1} - (y)_{j_e}]\{1 - \cos[(j-1)\pi/(N_y-1)]\}/2, \quad j = 1,2,3,\ldots,N_y, \tag{21}$$

where $i_e \in [1, I_E]$, $j_e \in [1, J_E]$, $i_e \times j_e = l$, $I_E \times J_E = N_E$, and $(x)_{i_e}, (x)_{i_e+1}, (y)_{j_e}$ and $(y)_{j_e+1}$ are the global x-and y-coordinates of the four edges of element l. Poisson's ratio has been taken to be $v = 0.3$.

Convergence studies are carried out first for the rectangular plate with mixed boundary conditions as shown in Fig. 2(a) and the cracked rectangular plate as shown in Fig. 2(c) to establish the minimum grid points required in each element for obtaining accurate solutions. The convergence patterns of the critical buckling factor p^2 with increasing number of grid points in each element are presented in Figs. 3 and 4. The completely converged buckling factor p_c^2 (to four significant digits) has been used to normalize the numerical results in these figures.

It is observed from Figs. 3 and 4 that, as the number of grid points in each element increases, the buckling factors converge to stable values. When the number of grid points in each element is smaller than 9×9, the convergence rate may vary slightly for different plate configurations and different relative thicknesses. However, when the mesh size for each element was greater than 9×9, all the buckling factors converged monotonically to the converged values very rapidly. A converged solution for the buckling factor to at least four significant figures could always be achieved when the mesh size for each element becames 13×13 regardless of the plate configuration and the relative thickness ratio h/a. In order to ensure high accuracy of the present solutions, 13×13 grid points in each element were therefore employed to generate all the numerical results in the following studies. To validate the accuracy of the solution method,

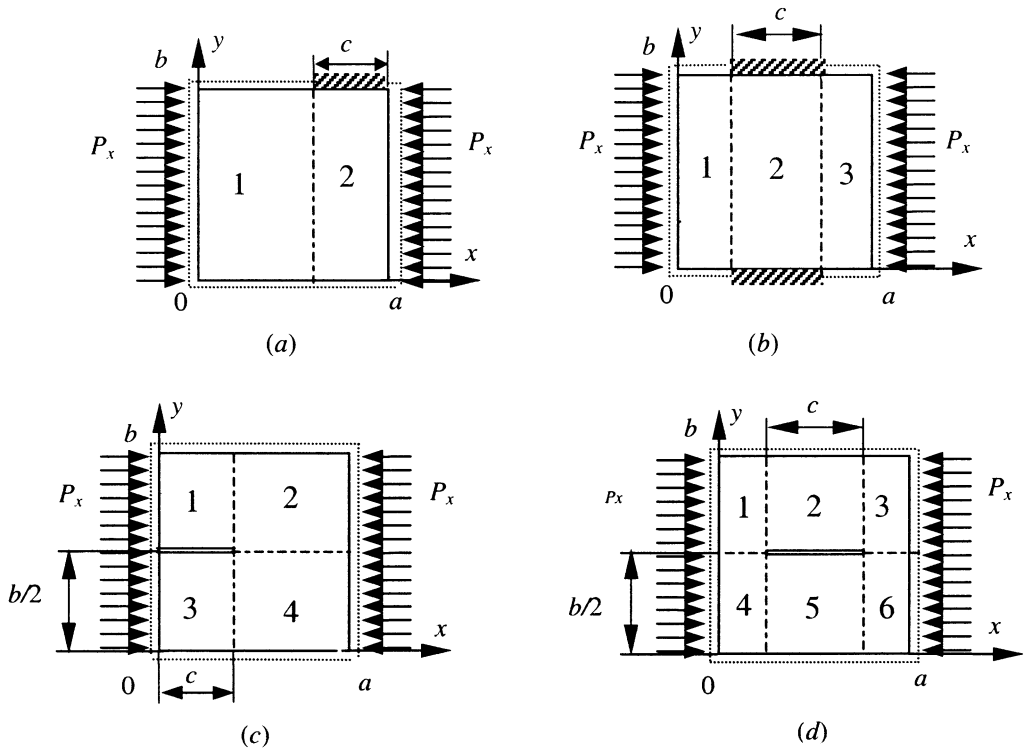

Fig. 2. Configurations of the rectangular Mindlin plates with different discontinuities analyzed by the present numerical methods.

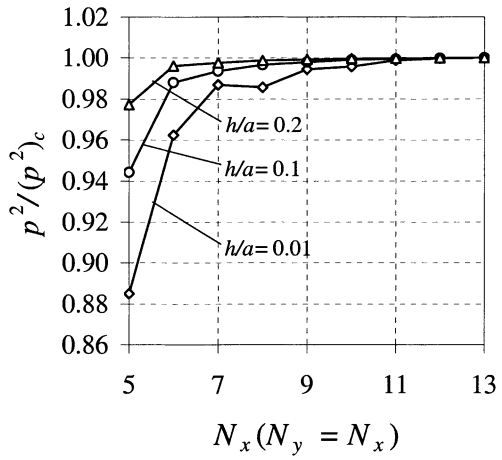

Fig. 3. Convergence of the buckling factor, $p^2 = P_x b^2/(\pi^2 D)$, with increasing number of grid points in each element for rectangular plate with mixed boundary conditions as shown in Fig. 2(a).

some comparitive studies were carried out in Tables 1 and 2. It should be noted that, in order to make a direct comparison of present DQEM results with other solutions, the value of the shear correction factor κ was taken to be 5/6 in both tables. In Table 1, a comparison of the present differential quadrature element method solutions with existing exact and numerical solutions for a square plate with different relative

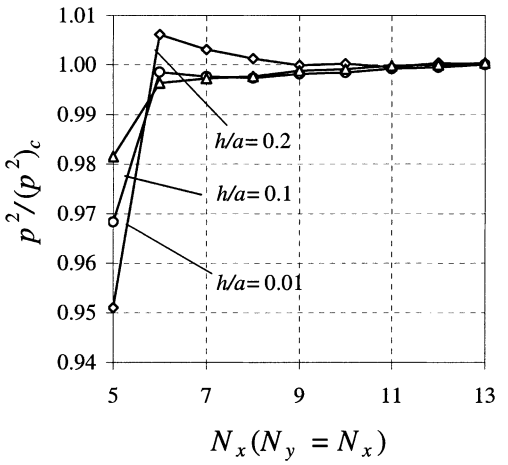

Fig. 4. Convergence of the buckling factor, $p^2 = P_x b^2/(\pi^2 D)$, with increasing number of grid points in each element for the cracked rectangular plate as shown in Fig. 2(c).

Table 1
Comparison studies of buckling factors $p^2 = P_x b^2/(\pi^2 D)$ for a square plate under uniaxial loading P_x

Boundary conditions	Sources	h/a			
		0.01	0.05	0.1	0.2
SSSS	Present	3.99775	3.94439	3.78645	3.26373
	Finite strip solution[a]	–	3.944	3.786	3.264
	p-Ritz method[b]	–	3.944	3.786	3.264
	Rayleigh-Ritz method[c]	–	3.929	3.731	–
	Exact 3-D solution[d]	–	3.911	3.741	3.150
	Thin plate solution	4.000	–	–	–
CCCC	Present	10.05204	9.55865	8.29165	5.31561
	p-Ritz method[b]	–	9.5588	8.2917	5.3156

[a] Hinton (1978).
[b] Xiang (1993).
[c] Dawe and Roufaeil (1982).
[d] Srinivas and Rao (1969).

Table 2
Comparison studies of buckling factors $p^2 = P_x b^2/(\pi^2 D)$ for a rectangular plate under different loading and boundary conditions

Boundary conditions	Loading conditions	h/b	Sources	a/b				
				1.0	1.25	1.50	1.75	2.0
SFSF	Uniaxial (P_x)	0.1	Present	0.92222	0.59129	0.41024	0.30091	0.22999
			p-Ritz method[a]	0.9223	0.5913	0.4103	0.3009	0.2296
		0.15	Present	0.89083	0.57787	0.40357	0.29724	0.22781
			p-Ritz method[a]	0.8908	0.5779	0.4036	0.2972	0.2278
SSSS	Biaxial ($P_x = P_y$)	0.1	Present	1.89323	1.56751	1.38791	1.2787	1.20744
			p-Ritz method[a]	1.893	1.568	1.388	1.279	1.207
			Finite strip solution[b]	1.893	1.568	1.388	1.279	1.207

[a] Xiang (1993).
[b] Hinton (1978).

thicknesses under uniaxial loading is presented. It is evident in this table that the present solutions are almost identical to the finite strip method solutions (Hinton, 1978) and the p-Ritz method solutions (Xiang, 1993) for both the SSSS and the CCCC plates. Table 2 shows the comparison of the present numerical solutions with the finite strip method solutions (Hinton, 1978) and p-Ritz method solutions (Xiang, 1993) for the buckling factors of a rectangular plate under different loading and boundary conditions. Different relative thicknesses and aspect ratios are considered. Again, excellent agreement has been observed. Thus, the reliability of the present solution has been confirmed.

4. Numerical examples and discussion

The numerical procedures presented in the previous sections can be employed to analyze buckling problems for a variety of Mindlin plates with different discontinuities such as a crack, a cut-out, stepped thickness, mixed boundary conditions, and discontinuities in the material properties. In this section, however, we only select four numerical examples to illustrate the validity and generality of the differential quadrature element method for solving such problems. All of these example plates are not solvable directly by using the global differential quadrature method but can be solved very easily by the present solution procedure. Some of the numerical results, where possible, are compared with the existing exact solutions to further verify the present solutions.

4.1. Rectangular plates with mixed boundary conditions

The first two example plates are rectangular plates with mixed boundary conditions. The geometry and loading conditions are shown in Fig. 2(a) and (b). The element divisions for these two plates are 2 and 3, respectively. Table 3 presents the numerical results for the buckling factors of a simply supported rectangular Mindlin plate with one edge partially clamped under uniaxial loading as shown in Fig. 2(a). For the thin plate ($h/a = 0.01$), the present solutions have been compared with the thin plate solutions obtained by Keer and Stahl (1972). Very good agreement is observed. The influences of the clamping ratio, c/a, and the plate relative thickness, h/a, on the buckling factor have also been investigated in this table. It is found that, as the clamping ratio c/a increases from 0.0 to 1.0, the buckling factor increases for all the relative thicknesses h/a ranging from 0.01 to 0.2. For a fixed value of clamping ratio c/a, the buckling factor decreases with increasing relative thickness. The variation of the buckling factor with the plate aspect ratio

Table 3
Buckling factors $p^2 = P_x b^2/(\pi^2 D)$ for a simply supported rectangular plate partially clamped along one edge under uniaxial loading P_x (Fig. 4(a))

a/b	c/a	$h/a = 0.01$		$h/a = 0.1$	$h/a = 0.2$
		p^2	Exact[a]	p^2	p^2
1.0	1/6	4.14000	4.1494	3.88529	3.34302
	1/3	4.52279	4.5454	4.18289	3.51687
	1/2	5.05548	5.0895	4.61400	3.77078
	2/3	5.5464	5.5696	5.04321	4.03651
	5/6	5.72147	5.7312	5.22863	4.19160
2.0	1/6	4.17038	–	3.36504	1.97187
	1/3	4.32591	–	3.43821	1.97498
	1/2	4.35255	–	3.47177	1.98387
	2/3	4.67170	–	3.54030	1.99117
	5/6	5.43352	–	3.78097	2.00811

[a] Exact solution obtained by Keer and Stahl (1972) based on thin plate theory.

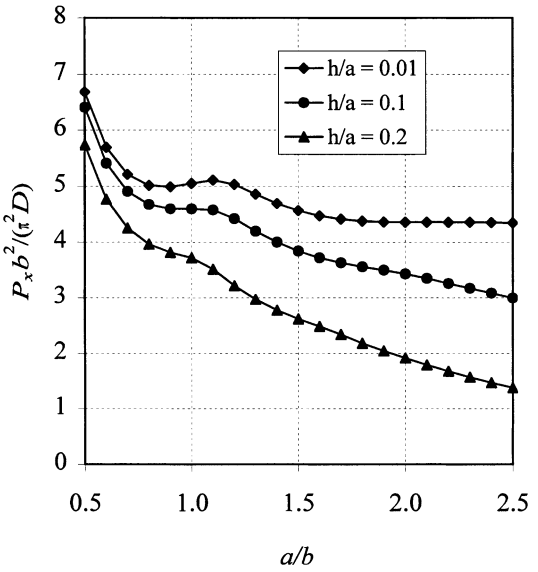

Fig. 5. Variation of the buckling factor, $p^2 = P_x b^2/(\pi^2 D)$, versus the aspect ratio, a/b, for a simply supported rectangular Mindlin plate partially clamped along one side of plate (Fig. 2(a), $c/a = 0.5$).

a/b is illustrated in Fig. 5. It is seen that the buckling factors decrease first and then shift to another buckling mode as the aspect ratio a/b increases.

Table 4 presents the numerical results for the buckling factors of a simply supported rectangular plate with the central portions of two opposite sides partially clamped under uniaxial compression as shown in Fig. 2(b). The analytical thin plate solutions given by Keer and Stahl (1972) are also listed in this table for comparison. The present results for the thin ($h/a = 0.01$) plate have been found in close agreement with existing values. The effects of the clamping ratio and the relative thickness on the buckling factor are similar

Table 4
Buckling factors $p^2 = P_x b^2/(\pi^2 D)$ for a simply supported rectangular plate partially clamped along central portions of two opposite edges under uniaxial loading P_x (Fig. 4(b))

a/b	c/a	$h/a = 0.01$		$h/a = 0.1$	$h/a = 0.2$
		p^2	Exact[a]	p^2	p^2
1.0	0.125	6.11948	6.2500	5.20788	4.07805
	0.250	6.54553	6.6152	5.65770	4.12740
	0.375	6.88077	6.9485	5.85695	4.20472
	0.500	7.22780	7.2900	6.08482	4.29485
	0.625	7.49234	7.5350	6.27687	4.37208
	0.750	7.63028	7.6563	6.39126	4.41844
2.0	0.125	4.14245	4.2353	3.34346	1.98928
	0.250	4.56438	4.6570	3.52109	1.99094
	0.375	5.01977	5.0625	3.61115	1.99554
	0.500	5.45498	5.5272	3.74478	2.00456
	0.625	6.10066	6.1951	3.96056	2.01682
	0.750	6.68306	6.7600	4.17377	2.03402

[a] Exact solution obtained by Keer and Stahl (1972) based on thin plate theory.

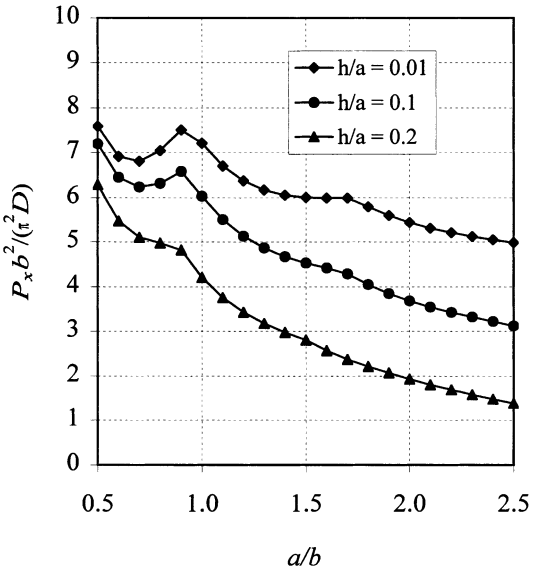

Fig. 6. Variation of the buckling factor, $p^2 = P_x b^2/(\pi^2 D)$, versus the aspect ratio, a/b, for a simply supported rectangular Mindlin plate with central portions of two opposite sides clamped (Fig. 2(b), $c/a = 0.5$).

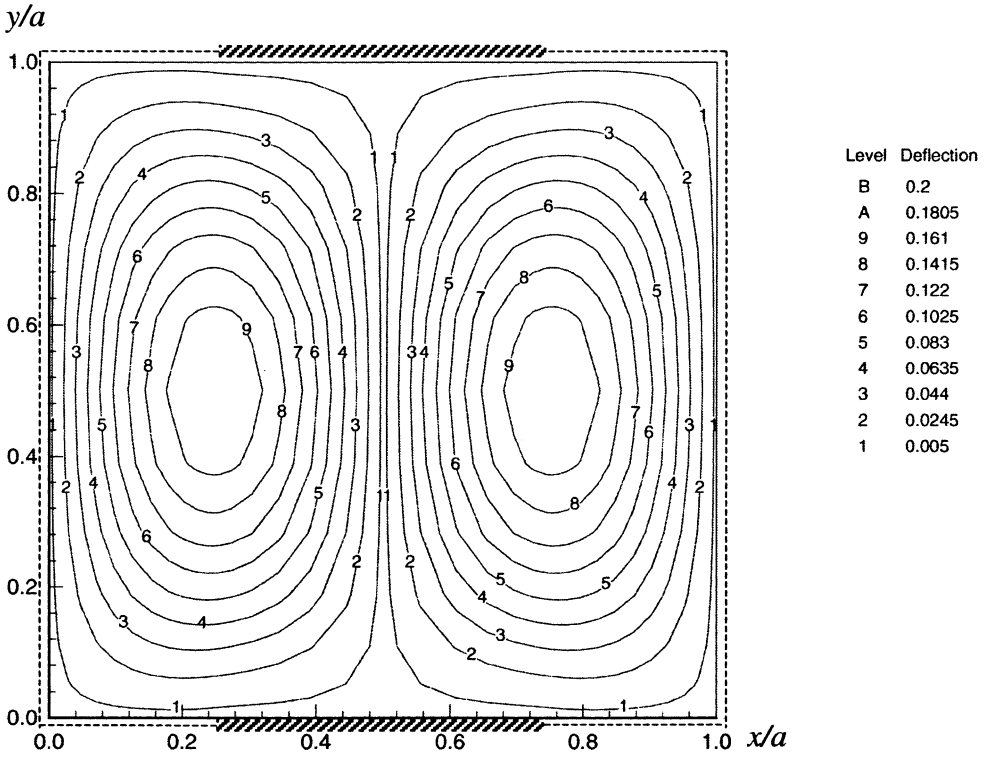

Fig. 7. Contour plot of buckling deflection mode shape for a simply supported rectangular plate with the central portions of two opposite sides partially clamped under uniaxial compression (Fig. 2(b), $c/a = 0.5$ and $h/a = 0.1$).

to those concluded in Table 3. However, the shifting of the buckling modes with increasing aspect ratio for the second example plates are more obviously observed from Fig. 6 than for the first example plate shown

Table 5
Buckling factors $p^2 = P_x b^2/(\pi^2 D)$ for a simply supported rectangular plate having a side crack from one edge under uniaxial loading P_x (Fig. 4(c))

a/b	c/a	$h/a = 0.01$		$h/a = 0.1$	$h/a = 0.2$
		p^2	Exact[a]	p^2	p^2
1.0	0.10	3.99473	–	3.79376	3.29126
	0.20	3.96101	–	3.76705	3.26588
	0.30	3.87079	–	3.67549	3.17860
	0.40	3.70818	–	3.49220	3.00966
	0.50	3.48642	–	3.24607	2.79715
	0.60	3.24614	–	2.99374	2.58902
	0.70	3.02643	–	2.77441	2.41142
	0.80	2.85355	–	2.60870	2.27823
	0.90	2.74484	–	2.50952	2.19915
2.0	0.10	3.97327	3.9920	3.27659	1.95176
	0.20	3.79608	3.8573	3.07325	1.85960
	0.30	3.40056	3.4633	2.70786	1.73809
	0.40	3.01143	3.0415	2.41210	1.63898
	0.50	2.72067	2.7291	2.20484	1.56491
	0.60	2.50994	2.5059	2.05829	1.51121
	0.70	2.34242	2.3348	1.94332	1.47167
	0.80	2.18237	2.1697	1.83189	1.43595
	0.90	2.02843	2.1963	1.72122	1.38835

[a] Exact solution obtained by Stahl and Keer (1972) based on thin plate theory.

Table 6
Buckling factors $p^2 = P_x b^2/(\pi^2 D)$ for a simply supported rectangular plate having a central crack under uniaxial loading P_x (Fig. 4(d))

a/b	c/a	$h/a = 0.01$		$h/a = 0.1$	$h/a = 0.2$
		p^2	Exact[a]	p^2	p^2
1.0	0.10	3.94976	3.9561	3.71157	3.21592
	0.20	3.81427	3.8259	3.53879	3.05796
	0.30	3.62432	3.6366	3.32643	2.86988
	0.40	3.41370	3.4225	3.11034	2.68535
	0.50	3.21064	3.2113	2.91454	2.52288
	0.60	3.03341	3.0241	2.75160	2.39055
	0.70	2.89167	2.8730	2.62674	2.29093
	0.80	2.78990	2.7622	2.54141	2.22383
	0.90	2.73001	2.6962	2.49460	2.18703
2.0	0.10	3.98628	–	3.29152	1.92721
	0.20	3.94834	–	3.17326	1.85438
	0.30	3.81076	–	2.88093	1.77657
	0.40	3.32145	–	2.58793	1.70716
	0.50	2.90674	–	2.32464	1.64369
	0.60	2.57041	–	2.09767	1.57787
	0.70	2.30654	–	1.91241	1.50304
	0.80	2.11441	–	1.77699	1.42818
	0.90	1.99777	–	1.69866	1.37550

[a] Exact solution obtained by Stahl and Keer (1972) based on thin plate theory.

in Fig. 5. The displacement contour plot for the buckling mode shape of the square plate with the clamping ratio $c/a = 0.5$ as shown in Fig. 2(b) is given in Fig. 7. The variation of the transverse deflection on the whole plate including the discontinuous points has been clearly demonstrated. It is found that the buckling mode shape is symmetrical about the two central lines of the plate.

4.2. Rectangular plates with cracks

To demonstrate the validity of the differential quadrature element method in solving the buckling of rectangular Mindlin plates with cracks, two more example plates, as shown in Fig. 2(c) and (d), are analyzed. The plate element divisions for computations are 2×2 for the rectangular plate with a side crack penetrating from the left side (Fig. 2(c)) and 3×2 for the rectangular plate with a centrally located crack (Fig. 2(d)), respectively. The numerical results have been given in Tables 5 and 6 together with the thin plate solutions obtained by Stahl and Keer (1972). The present results for the thin ($h/a = 0.01$) plates are all in good agreement with the existing solutions in both tables. It is discovered in Tables 5 and 6 that the critical buckling factors decrease as the relative crack length c/a increases. This is reasonable since the plate stiffness reduces when the crack length increases. The effect of the relative thickness on the buckling factor is similar to that shown in the previous two cases. Fig. 8 shows the variations of the buckling factors with the plate aspect ratio a/b for the cracked rectangular plate shown in Fig. 2(c). Compared to the buckling solutions in Figs. 5 and 6, one may find that the variation of the buckling factors versus the plate aspect ratio in Fig. 8 is different from the previous two examples. The buckling factors decrease monotonically as the aspect ratio increases, and the mode shift points are not easily distinguished in this case. In order to examine the variation of the deflection on the entire plate with a crack, the buckling mode shape for the square plate having a side crack with $c/a = 0.5$ (Fig. 2(c)) is presented in Fig. 9. It is

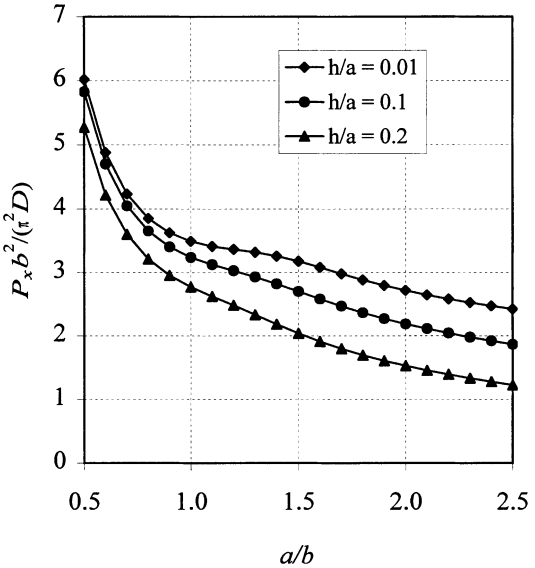

Fig. 8. Variation of the buckling factor, $p^2 = P_x b^2/(\pi^2 D)$, versus the aspect ratio, a/b, for a simply supported rectangular Mindlin plate having a side crack from the edge $x = 0$ (Fig. 2(c), $c/a = 0.5$).

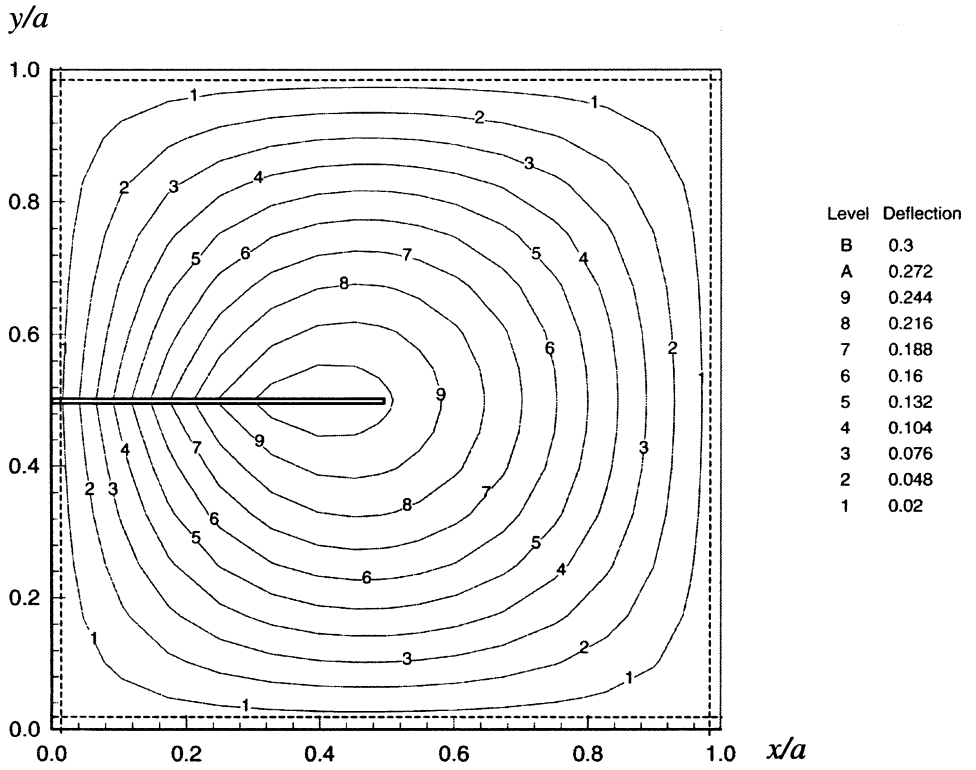

Fig. 9. Contour plot of buckling deflection mode shape for a simply supported square plate having a side crack from the edge $x = 0$ under uniaxial compression (Fig. 2(c), $c/a = 0.5$ and $h/a = 0.1$).

evident that the transverse displacement is symmetrical about the central line of the plate parallel to the x-axis.

5. Conclusion

In this paper, the two-dimensional differential quadrature element method has been applied to the buckling analysis of Mindlin plates based on the differential quadrature method and the domain decomposition method. The reliability of the methodology has been established through convergence and accuracy studies, and through comparison studies with existing analytical solutions. Four example plates with different discontinuities, which are not solvable by the global differential quadrature method, have been analyzed successfully by the present differential quadrature element method to demonstrate the applicability and versatility of the method for practical purposes. The effects of the relative lengths of the discontinuities (relative clamping ratio and crack ratio), the plate thickness, and the plate aspect ratio on the buckling factors for these example plates have been investigated. The numerical results for the thin ($h/a = 0.01$) plates have been compared with the existing exact solutions to further validate the present numerical solutions. It is found that the differential quadrature element method is an effective solution approach for the title problem, with both high accuracy and great flexibility.

References

Bellman, R.E., Casti, J., 1971. Differential quadrature and long term integration. J. Math. Anal. Appl. 34, 235–238.

Bellman, R.E., Kashef, B.G., Casti, J., 1972. Differential quadrature: a technique for the rapid solution of non-linear partial differential equations. J. Computat. Phys. 10, 40–52.

Bert, C.W., Jang, S.K., Striz, A.G., 1988. Two new approximate methods for analyzing free vibration of structural components. AIAA J. 26, 612–618.

Bert, C.W., Jang, S.K., Striz, A.G., 1989. Nonlinear bending analysis of orthotropic rectangular plates by the method of differential quadrature. Computat. Mech. 5, 217–226.

Bert, C.W., Malik, M., 1996. Differential quadrature method in computational mechanics: a review. Appl. Mech. Rev. 49, 1–28.

Brunelle, E.J., 1971. Buckling of transversely isotropic Mindlin plates. AIAA J. 9, 1018–1022.

Brunelle, E.J., Robertson, S.R., 1974. Initially stressed Mindlin plates. AIAA J. 12, 1036–1045.

Chen, W., Striz, A.G., Bert, C.W., 1997. A new approach to the differential quadrature method for fourth-order equations. Int. J. Numer. Meth. Engng. 40, 1941–1956.

Dawe, D.J., Roufaeil, O.L., 1982. Buckling of rectangular Mindlin plates. Comput. Struct. 15, 461–471.

Hamada, M., Inoue, Y., Hashimoto, H., 1967. Buckling of simply supported but partially clamped rectangular plates uniformly compressed in one direction. Bull. JSME 10, 35–40.

Han, J.-B., Liew, K.M., 1996. The differential quadrature element method (DQEM) for axisymmetric bending of thick circular plates. Proc. of the Third Asian-Pacific Conf. on Comput. Mech. pp. 2363–2368.

Hinton, E., 1978. Buckling of initially stressed Mindlin plates using a finite strip method. Comput. Struct. 8, 99–105.

Keer, L.M., Stahl, B., 1972. Eigenvalue problems of rectangular plates with mixed edge conditions. Trans. ASME J. Appl. Mech. 39, 513–520.

Leissa, A.W., 1995. Buckling and postbuckling theory for laminated composite plates. In: Turvey, G.J., (Ed.), Buckling and Postbuckling of Composite Plates. Chapman and Hall, London. pp. 22–26.

Liew, K.M., Han, J.-B., Xiao, Z.M., Du, H., 1996. Differential quadrature method for Mindlin plates on Winkler foundations. Int. J. Mech. Sci. 38, 405–421.

Liu, F.-L., Liew, K.M., 1998. Static analysis of Reissner-Mindlin plates by differential quadrature element method. Trans. ASME J. Appl. Mech. 65, 705–710.

Liu, F.-L., Liew, K.M., 1999a. Differential quadrature element method for static analysis of Reissner-Mindlin polar plates. Int. J. Solids Struct. 36 (33), 5101–5123.

Liu, F.-L., Liew, K.M., 1999b. Vibration analysis of discontinuous Mindlin plates by differential quadrature element method. Trans. ASME J. Vibr. Acoust. 121, 204–208.

Liu, F.-L., Liew, K.M., 1999c. Differential quadrature element method: a new approach for free vibration analysis of polar Mindlin plates having discontinuities. Comput. Meth. Appl. Mech. Engng. 179 (3–4), 407–423.

Liu, F.-L., 2000. Rectangular plates on Winkler foundation: differential quadrature element solution. Int. J. Solids Struct. 37, 1743–1763.

Luo, J.-W., 1982. A hybrid/mixed model finite element analysis for buckling of moderately thick plates. Comput. Struct. 15, 359–364.

Malik, M., Bert, C.W., 1998. Three-dimensional elasticity solutions for free vibrations of rectangular plates by the differential quadrature method. Int. J. Solids Struct. 35, 299–381.

Mindlin, R.D., 1951. Influence of rotatory inertia and shear on flexural motion of isotropic, elastic plates. Trans. ASME J. Appl. Mech. 18, 31–38.

Rao, V.G., Venkataramana, J., Raju, K.K., 1975. Stability of moderately thick rectangular plates using a high precision triangular finite element. Comput. Struct. 5, 257–259.

Reissner, E., 1945. The effect of transverse shear deformation on the bending of elastic plates. Trans. ASME J. Appl. Mech. 12, 69–77.

Sakiyama, T., Matsuda, H., 1987. Elastic buckling of rectangular Mindlin plates with mixed boundary conditions. Comput. Struct. (Technical Note) 25, 801–808.

Srinivas, S., Rao, A.K., 1969. Buckling of rectangular thick plates. AIAA J. 7, 1645–1746.

Stahl, B., Keer, L.M., 1972. Vibration and stability of cracked rectangular plates. Int. J. Solids Struct. 8, 69–92.

Striz, A.G., Jang, S.K., Bert, C.W., 1988. Non-linear bending analysis of thin circular plates by differential quadrature. Thin-Walled Struct. 69, 51–62.

Striz, A.G., Chen, W., Bert, C.W., 1994. Static analysis of structures by the quadrature element method. Int. J. Solids Struct. 31, 2807–2818.

Striz, A.G., Chen, W., Bert, C.W., 1997. Free vibration of high-accuracy plate elements by the quadrature element method. J. Sound Vibr. 202, 689–702.

Wang, X., Gu, H., 1997. Static analysis of frame structures by the differential quadrature element method. Int. J. Numer. Meth. Engng. 40, 759–772.

Whitney, J.M., 1987. Structural Analysis of Laminated Anisotropic Plates. Technomic, Lancaster, USA. pp. 265–270.
Wittrick, W.H., 1987. Analytical, three-dimensional elasticity solutions to some plate problems, and some observations on Mindlin's plate theory. Int. J. Solids Struct. 23, 441–464.
Xiang, Y., 1993. Numerical Developments in Solving the Buckling and Vibration of Mindlin Plates. Ph. D. thesis, The University of Queensland, Australia.